Dicopper(II) Complexes of the Antitumor Analogues Acylbis(salicylaldehyde hydrazones) and Crystal Structures of Monomeric $[Cu_2$(1,3-propanedioyl bis(salicylaldehyde hydrazone))$(H_2O)_2]\cdot(ClO_4)_2\cdot 3H_2O$ and Polymeric $[\{Cu_2$(1,6-hexanedioyl bis(salicylaldehyde hydrazone))$(C_2H_5OH)_2\}_m]\cdot(ClO_4)_{2m}\cdot m(C_2H_5OH)$

John D. Ranford,*,† Jagadese J. Vittal, and Yu M. Wang

Department of Chemistry, National University of Singapore, Lower Kent Ridge Road, Singapore 119260

Received June 26, 1997

Salicylaldehyde hydrazones derived from acyldicarboxylic acids (H_4L^n, where $n = 0$, 1, 2, 4, 6, 8, 10, 14 and is the number of methylene units) of varying chain length have been prepared, and their dicopper(II) complexes have been isolated as bis analogues of antitumor carboxylate hydrazones. The predominant structural form adopted is polymeric, with $[\{Cu_2L^n\}_m]$ formed in neutral or basic solution, $[\{Cu_2(H_2L^n)Cl_2\}_m]$ from dilute HCl, and $[\{Cu_2(H_2L^n)\}_m]\cdot(ClO_4)_{2m}$ from dilute $HClO_4$. The crystal structures of $[Cu_2(H_2L^1)(H_2O)_2]\cdot(ClO_4)_2\cdot 3H_2O$ and $[\{Cu_2(H_2L^4)(C_2H_5OH)_2\}_m]\cdot(ClO_4)_{2m}\cdot m(C_2H_5OH)$ have been determined. The structure of $[Cu_2(H_2L^1)(H_2O)_2]\cdot(ClO_4)_2\cdot 3H_2O$ consists of discrete di-Cu(II) molecules with nonsymmetry-related Cu(II) centers. The copper atoms are square-planar with H_2L^1 supplying two tridentate, monoanionic ONO domains and water completing the coordination sphere. The two metal-binding domains are inclined at 80° to each other. For $[\{Cu_2(H_2L^4)(C_2H_5OH)_2\}_m]\cdot(ClO_4)_{2m}\cdot m(C_2H_5OH)$ the symmetry-related copper atoms are square-pyramidal with the base composed of H_2L^4, acting as a tridentate ONO chelator, and an O-bonded ethanol molecule. Axial phenolato bridges complete the coordination sphere, linking molecules to give a polymer. Compounds prepared have been characterized by a range of physicochemical and spectroscopic techniques, and proton and metal ion stability constant data have been determined.

Introduction

Investigation into the iron-binding potential of a range of hydrazone derivatives,[1] as drugs for genetic disorders such as thalassemia, led to the discovery that salicylaldehyde benzoylhydrazone (H_2sb) inhibits DNA synthesis and cell growth.[2]

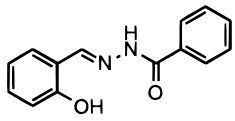

Salicylaldehyde

benzoylhydrazone - H_2sb

Intriguingly, the copper(II) complex was shown to be significantly more potent than the metal-free chelate, leading to the suggestion that the metal complex was the biologically active species. Prior to this, H_2sb was found to possess mild bacteriostatic activity.[3] Because of the biological interest in this type of chelate system, several structural studies have been carried out on copper[4−6] with H_2sb and analogues. This class of diprotic ligand typically acts as tridentate, planar chelates coordinating through the phenolic and amide oxygens and the imine nitrogen. The actual ionization state is dependent upon the conditions and metal employed.[6] With Cu(II) in base, both the phenolic and amide protons are ionized; in neutral and mild acidic solution the ligands are monoanionic, whereas strongly acidic conditions are necessary to form compounds formulated with a neutral ligand. Such copper(II) complexes often exhibit antiferromagnetism which may be due to the structurally observed preference for planar, phenolato bridged dimers.[5−7]

Acylhydrazones of salicylaldehyde subsequently attracted attention. Salicylaldehyde acetylhydrazone (H_2sa) displays radioprotective properties,[8] and a range of acylhydrazones have

† E-mail: chmjdr@nus.edu.sg.

(1) (a) Ponka, P.; Borova, J.; Neuwirth, J.; Fuchs, O. *FEBS Lett.* **1970**, *97*, 317−320. (b) Vitolo, M. L.; Webb, J. *J. Inorg. Biochem*. **1984**, *20*, 255−262. (c) Baker, E.; Vitolo, M. L.; Webb, J. *Biochim. Pharmacol*. **1985**, *34*, 3011−3017. (d) Ponka, P.; Richardson, D.; Baker, E.; Schulman, H. M.; Edward, J. T. *Biochim. Biophys. Acta* **1988**, *967*, 122−129.

(2) (a) Johnson, D. K.; Murphy, T. B.; Rose, N. J.; Goodwin, W. H.; Pickart, L. *Inorg. Chim. Acta* **1982**, *67*, 159−165. (b) Pickart, L.; Goodwin, W. H.; Burgua, W.; Murphy, T. B.; Johnson, D. K. *Biochem. Pharmacol*. **1983**, *32*, 3868−3871.

(3) Offe, H. A.; Siefken, W.; Domagk, G. *Z. Naturforsch.* **1952**, *7B*, 462−468.

(4) (a) Aruffo, A. A.; Murphy, T. B.; Johnson, D. K.; Rose, N. J.; Schomaker, V. *Acta Crystallogr., Sect. C* **1984**, *40*, 1164−1169. (b) Ainscough, E. W.; Brodie, A. M.; Dobbs, A.; Ranford, J. D.; Waters, J. M. *Inorg. Chim. Acta* **1995**, *236*, 83−88.

(5) Chan, S. C.; Koh, L. L.; Leung, P.-H.; Ranford, J. D.; Sim, K. Y. *Inorg. Chim. Acta* **1995**, *236*, 101−108.

(6) Ainscough, E. W.; Brodie, A. M.; Dobbs, A.; Ranford, J. D.; Waters, J. M. *Inorg. Chim. Acta* **1998**, *267*, 27−38.

(7) Moubaraki, B.; Murray, K. S.; Ranford, J. D.; Robinson, W. T.; Svensson, J.; Wu D. Q. Manuscript in preparation.

(8) Arapov, O. V.; Alferva, O. F.; Levocheskaya, E. I.; Krasil'nikov, I. *Radiobiologiya* **1987**, *27*, 843−846.

S0020-1669(97)00805-7 CCC: $15.00
Published on Web 02/26/1998

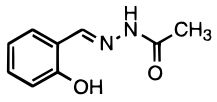

Salicylaldehyde

acetylhydrazone - H_2sa

been shown to be cytotoxic,[9] the copper complexes again showing enhanced activity. Little is known on the mechanisms of bioactivity for any of these compounds.

The natural extension from this is to acyldihydrazones (H_4L^n)- and predominantly synthetic studies on selective ranges of

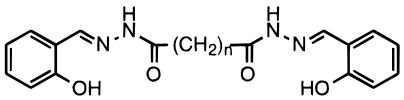

Salicylaldehyde acyldihydrazones - H_4L^n

ligands with transition metals have been carried out.[10] Nickel(II),[11] dioxomolybdenum(VI),[12] and dioxouranium(VI)[13] complexes have been prepared to investigate the ligating properties of the system. With Cu(II), complexes were isolated from the potentially hexadentate chelates either with one metal ion per ligand ($n = 0$)[14] and a normal magnetic moment or with two metal ions and low moments ($n = 0-4$).[15] Structures were proposed on the basis of spectroscopic and magnetic susceptibility data.

This paper reports the synthesis and characterization of an extended range of salicylaldehyde acyldihydrazone ligands (H_4L^n, $n = 0$, 1, 2, 4, 6, 8, 10, 14) and their dicopper(II) complexes formed from both neutral or basic ($[\{Cu_2L^n\}_m]$) and dilute acid solutions ($[\{Cu_2(H_2L^n)Cl_2\}_m]$ and $[\{Cu_2(H_2L^n)\}_m]\cdot(ClO_4)_{2m}$). The crystal structures of monomeric $[Cu_2(H_2L^1)(H_2O)_2]\cdot(ClO_4)_2\cdot 3H_2O$ and polymeric $[\{Cu_2(H_2L^4)(C_2H_5OH)_2\}_m]\cdot(ClO_4)_{2m}\cdot m(C_2H_5OH)$, the first for this ligand class with copper, are reported. Preliminary proton and copper(II) ion stability constant data have been determined for this system and for H_2as for comparison.

Experimental Section

Caution: *As these ligands are cytotoxic, they should be handled with necessary care.*

Ligand Preparations. Except for oxalate bis(salicylaldehyde hydrazone) (H_4L^0), which will be given separately, all ligands were prepared using a similar procedure; therefore, one general example will be given.

H_4L^n. To the diethyl ester of the diacid (37.6 mmol) in absolute ethanol (5 mL) was added hydrazine hydrate (7.29 mL, 150 mmol), and the solution refluxed for 10 h. The resulting white dihydrazide was filtered, given a cursory wash with ethanol, and then dried in vacuo. To a suspension of the dihydrazide (13.5 mmol) in ethanol (20 mL) was added salicylaldehyde (2.90 mL, 27.7 mmol), and the mixture was stirred in an ice bath for 8 h. The white precipitate of the desired dihydrazone was collected and washed with ethanol prior to drying in vacuo.

H_4L^0. The previous procedure was repeated using dimethyl ethandioate. However, after the addition of the salicylaldehyde, the reaction was stirred for 4 h as prolonged reaction results in a yellow coloration. The compound was recrystallized from DMF to give white product. Yield 57%; mp 321−322 °C (lit.[15] >250 °C); ^{1}H NMR [$(CD_3)_2$SO] δ 6.79−7.57 (m, 8H), 8.81 (s, 2H), 11.00 (s, 2H), 12.63 (s, 2H). Anal. Calcd (Found): C, 58.7 (58.9); H, 4.3 (4.3); N, 17.3 (17.2).

H_4L^1. Yield 84%; mp 234−236 °C (lit.[15] 230 °C); ^{1}H NMR [$(CD_3)_2$SO] (isomer **I** 50% + isomer **II** 50%), δ 3.61 + 3.90 (s, 2H), 6.8−7.7 (m, 8H), 8.42 + 8.43 (s, 2H), 11.40 (s, 4H), 12.63 (s, 2H). Anal. Calcd (Found): C, 60.0 (60.0); H, 4.6 (4.7); N, 16.5 (16.5).

H_4L^2. Yield 65%; mp 273−275 °C (lit.[15] 230 °C); ^{1}H NMR [$(CD_3)_2$SO] (isomer **I** 41% + isomer **II** 22% + isomer **III** 22% + isomer **IV** 15%), 2.55 (t) + 2.58 (s) + 2.91 (s) + 2.93 (t) (4H), 6.8−7.7 (m, 8H), 8.27 + 8.28 + 8.35 (s, 2H), 11.16 + 11.20 + 11.26 + 11.28 (s, 2H), 10.13 + 11.68 + 11.70 (s, 2H). Anal. Calcd (Found): C, 61.0 (61.0); H, 5.0 (5.1); N, 15.7 (15.8).

H_4L^4. Yield 76%; mp 300−302 °C (lit.[15] >250 °C); ^{1}H NMR [$(CD_3)_2$SO] (isomer **I** 67% + isomer **II** 33%), δ 1.63 (t, 4H), 2.26 + 2.62 (t, 4H), 6.8−7.7 (m, 8H), 11.19 (s, 2H), 11.60 + 10.12 (s, 2H). Anal. Calcd (Found): C, 62.6 (62.8); H, 5.8 (5.8); N, 14.3 (14.6).

H_4L^6. Yield 55%; mp 220−223 °C; ^{1}H NMR [$(CD_3)_2$SO] (isomer **I** 67% + isomer **II** 33%), δ 1.33 (m, 4H), 1.59 (m, 4H), 2.22 + 2.57 (t, 4H), 6.8−7.7 (m, 8H), 8.33 + 8.25 (s, 2H), 11.18 (s, 2H), 11.56 + 11.14 (s, 2H). Anal. Calcd (Found): C, 64.1 (64.4); H, 6.6 (6.4); N, 13.7 (13.7).

H_4L^8. Yield 71%; mp 206−208 °C (lit.[11] 213−4 °C); ^{1}H NMR [$(CD_3)_2$SO] (isomer **I** 67% + isomer **II** 33%), δ 1.29 (m, 8H), 1.58 (m, 4H), 2.21 + 2.56 (t, 4H), 6.8−7.7 (m, 8H), 8.33 + 8.24 (s, 2H), 11.20 + 11.17 (s, 2H), 11.57 + 10.12 (s, 2H). Anal. Calcd (Found): C, 65.6 (65.7); H, 6.9 (6.9); N, 12.9 (12.8).

H_4L^{10}. Yield 87%; mp 231−232 °C; ^{1}H NMR [$(CD_3)_2$SO] (isomer **I** 67% + isomer **II** 33%), δ 1.27 (m, 12H), 1.57 (m, 4H), 2.20 + 2.55 (t, 4H), 6.8−7.7 (m, 8H), 8.33 + 8.24 (s, 2H), 11.20 + 11.17 (s, 2H), 11.55 + 10.12 (s, 2H). Anal. Calcd (Found): C, 66.5 (66.9); H, 7.3 (7.3); N, 12.2 (12.0).

H_4L^{14}. Yield 88%; mp 160−162 °C; ^{1}H NMR [$(CD_3)_2$SO] (isomer **I** 67% + isomer **II** 33%), δ 1.24 (m, 20H), 1.57 (m, 4H), 2.21 + 2.51 (t, 4H), 6.8−7.7 (m, 8H), 8.34 + 8.25 (s, 2H), 11.19 + 11.16 (s, 2H), 11.54 + 10.13 (s, 2H). Anal. Calcd (Found): C, 68.7 (68.9); H, 8.2 (8.1); N, 10.7 (10.7).

Complex Preparations. A general procedure will be given for each type of complex prepared.

Warning: Perchlorate salts are potentially explosive.

$[\{Cu_2L^n\}_m]\cdot x m H_2O$. To a hot solution of the ligand (0.5 mmol) in DMF (10 mL) (for H_4L^{14} the solvent was 1:3 DMF/ethanol, 20 mL) was added LiOH (48 mg, 2.0 mmol) in water (5 mL). $CuCl_2\cdot 2H_2O$ (176 mg, 1.03 mmol) in absolute ethanol (7 mL) was added dropwise to the resulting yellow solution. The precipitate that formed was stirred for 2 h with gentle heating, filtered, and then washed successively with water, ethanol, and diethyl ether prior to drying in vacuo. Yields ranged from 47 to 94%.

$[\{Cu_2(H_2L^n)Cl_2\}_m]\cdot x m H_2O$. Two drops of concentrated HCl were added to a hot solution of the ligand (0.5 mmol) in DMF (10 mL). To this was added $CuCl_2\cdot 2H_2O$ (176 mg, 1.03 mmol) in absolute ethanol (7 mL), and the dark green solution that formed was left to evaporate until the brown or yellow-green precipitate appeared. The product was filtered, washed successively with acidified (HCl) ethanol and diethyl ether, and dried in vacuo. Yields ranged from 22 to 37%.

$[\{Cu_2(H_2L^n)(H_2O)_2\}_m]\cdot(ClO_4)_{2m}\cdot x m H_2O$. To a suspension of the ligand (0.5 mmol) in ethanol (25 mL) was added $Cu(ClO_4)_2\cdot 6H_2O$ (382

(9) Koh, L. L.; Kuan, W. L.; Lian, K. O.; Long, Y. C.; Ranford, J. D.; Tan, L. C.; Tjan, Y. Y., Submitted.

(10) (a) Umarov, B. B.; Khusenov, K. S.; Ishankhodzhaeva, M. M.; Parpiev, N. A.; Gaibullaev, K. S. *Zh. Org. Khim.* **1996**, *32*, 93−95. (b) Aggarawal, R. C.; Singh, B. *Curr. Sci.* **1978**, *47*, 679−680. (c) Narang, K. K.; Lal, R. A. *Transition Met. Chem. (London)* **1977**, *2*, 100−103. (d) Zhang, X.-M.; You, X.-Z. *Polyhedron* **1996**, *15*, 1793−1796.

(11) Sacconi, L. *J. Chem. Soc.* **1954**, *Part I*, 1326−1328.

(12) (a) Wang, X.; Zhang, X. M.; Liu, H. X. *Polyhedron* **1994**, *13*, 2611−2614. (b) Wang, X.; Zhang, X. M.; Liu, H. X. *Acta Crystallogr., Sect. C* **1994**, *50*, 1878−1880.

(13) (a) Lal, R. A.; Das, S.; Thapa, R. K. *Inorg. Chim. Acta* **1987**, *132*, 129−136. (b) Das, S.; Lal, R. A. *Indian J. Chem.* **1988**, *27A*, 225−230. (c) Husain, M.; Bhattacharjee, S. S.; Singh, K. B.; Lal, R. A. *Polyhedron* **1991**, *10*, 779−788.

(14) Narang, K. K.; Lal, R. A. *Curr. Sci.* **1977**, *46*, 401−403.

(15) Lal, R. A.; Srivastava, K. N.; Das, S. *Synth. React. Inorg. Met.−Org. Chem.* **1988**, *18*, 837−848.

mg, 1.03 mmol) followed by 70% $HClO_4$ (0.5 mL). The resulting emerald solution was refluxed for 1.5 h, filtered, and then left to evaporate at room temperature. The product was collected after ca. 1 week and given a cursory wash with ethanol and then diethyl ether prior to drying in vacuo. Yields were ca. 40%.

X-ray Crystallography. 1. $[Cu_2(H_2L^1)(H_2O)_2]\cdot(ClO_4)_2\cdot 3H_2O$. (a) Crystal Data. $C_{17}H_{24}Cl_2Cu_2N_4O_{17}$, monoclinic, space group $P2_1/n$, a = 9.7447(1) Å, b = 21.1248(2) Å, c = 16.2286(2) Å, β = 95.034(1)°, U = 3327.85(6) Å^3, Z = 4, M = 750.35 g mol^{-1}, D_c = 1.498 g cm^{-3}, absorption coefficient, 1.509 mm^{-1}, λ = 0.710 73 Å, $F(000)$ = 1512, crystal dimensions, 0.40 × 0.33 × 0.23 mm.

(b) Measurements. Data were collected at 23 °C on a Siemens SMART CCD diffractometer with Mo Kα radiation (λ = 0.710 73 Å) with the crystal sealed in a glass capillary tube. Preliminary cell constants were obtained from 45 frames of data (width of 0.3° in ω). Final cell parameters were obtained by global refinements of reflections obtained from integration of all the frame data. A total of 16 598 reflections were collected in the θ range 1.59−25.0° (h = −13 to 13; k = −20 to 27; l = −17 to 21) with a frame width of 0.3° in ω and a counting time of 20 s per frame at a crystal-to-detector distance of 4.095 cm. The collected frames were integrated using the preliminary cell-orientation matrix. The software used were SMART[16] for collecting frames of data, indexing reflections, and determination of lattice parameters; SAINT[16] for integration of intensity of reflections and scaling; SADABS[17] for absorption correction; and SHELXTL[18] for space group and structure determination, refinements, graphics, and structure reporting.

(c) Structural Analysis. The space group $P2_1/n$ was determined from the systematic absences. All the non-hydrogen atoms in the neutral molecules were refined anisotropically. The two ClO were severely disordered. For one perchlorate anion the two ClO_3 fragments were anchored on a common oxygen atom O(1A). In the second perchlorate anion, three independent ClO_4 disorder models were included. The occupancies 0.4, 0.4, and 0.2 were arbitrary and were not refined. Common isotropic thermal parameters were refined for the first two fragments, and the thermal parameter was fixed at 0.08 for the third one. The option SADI was used to apply soft constraints on the Cl−O and O···O distances for ClO_4 fragments containing Cl(1) and Cl(1A). Ideal geometry was imposed on the other perchlorate anion using the option DFIX. About 3 water molecules were found in the crystal lattice. They were severely disordered, too, and sixteen positions were found in the difference Fourier routine. The occupancy ranges from 0.25 to 0.125. No hydrogen atoms were added for these solvent oxygens atoms. However, individual isotropic thermal parameters were refined. The hydrogen atoms of the C's and N's were placed in the ideal positions using riding models. In the final least-squares refinement cycles on F^2, the model converged at R_1 = 0.0752, wR_2 = 0.2322, and GOF = 1.026 for 4628 reflections with $F_o > 4\sigma(F_o)$ and 416 parameters, and R_1 = 0.0922 and wR_2 = 0.2477 for all 5779 data. In the final difference Fourier synthesis the electron density fluctuates in the range 0.73 to −2.26 e Å^{-3}. The top 11 peaks were associated with either disordered ClO_4 or with solvent molecules. In the final cycle, the maximum shift and shift/esd are 0.080 and 0.003, respectively. An extinction correction was refined to 0.0003(5). The positional and thermal parameters are given in the Supporting Information. Severe disorder present in the anions and the solvents are attributed to the poor agreement factors. However, the connectivities of the atoms in the cation are well established in this study.

2. $[\{Cu_2(H_2L^4)(C_2H_5OH)_2\}_m]\cdot(ClO_4)_{2m}\cdot m(C_2H_5OH)$. (a) Crystal Data. $C_{26}H_{38}Cl_2Cu_2N_4O_{15}$, triclinic, space group $P\bar{1}$, a = 7.9024(1) Å, b = 10.6596(1) Å, c = 11.0574(1) Å, α = 73.664(1)°, β = 86.210(1)°, γ = 87.668(1)°, U = 891.64(2) Å^3, Z = 1, M = 844.58 g mol^{-1}, D_c = 1.573 g cm^{-3}, absorption coefficient, 1.41 mm^{-1}, λ = 0.710 73 Å, $F(000)$ = 434, crystal dimensions, 0.5 × 0.5 × 0.4 mm.

(b) Measurements. Data were collected at 23 °C on a Siemens SMART CCD diffractometer with Mo Kα radiation (λ = 0.710 73 Å), with the crystal sealed in a glass capillary tube. Preliminary cell constants were obtained from 45 frames of data (width of 0.3° in ω). Final cell parameters were obtained by global refinements of reflections obtained from integration of all the frame data. A total of 5459 reflections were collected in the θ range 1.92−29.02° (h = −5 to 10; k = −13 to 13; l = −14 to 14) with a frame width of 0.3° in ω and a counting time of 20 s per frame at a crystal-to-detector distance of 5.027 cm. Data treatment was as for the previous structure.

(c) Structural Analysis. The space group $P\bar{1}$ was chosen in the triclinic system and for Z = 1, a crystallographic inversion center was imposed. All the non-hydrogen atoms except the oxygens of the ClO were refined anisotropically. The perchlorate oxygen atoms were disordered, and four different sets of orientations (occupancies of 0.3, 0.3, 0.2, and 0.2) were found in the difference Fourier maps. Attempts to refine the anisotropic thermal parameters of the O atoms were not satisfactory, therefore common isotropic thermal parameters were assigned for each set of oxygen atoms and were refined. The carbon atoms of the two ethanol molecules showed relatively high thermal parameters. The nonbonded ethanol molecule is disordered by virtue of its crystallographic symmetry. All H atoms were located successfully. The positional and isotropic thermal parameter of the H atom attached to O(3) was refined, and a riding model was used to place the rest of the hydrogen atoms in their idealized positions. In the final least-squares refinement cycles on F^2, the model converged at R_1 = 0.0587, wR_2 = 0.1700, and GOF = 1.096 for 3623 reflections with $F_o > 4\sigma(F_o)$ and 259 parameters, and R_1 = 0.0627 and wR_2 = 0.1741 for all 4017 data. In the final difference Fourier synthesis the electron density fluctuates from 1.23 to −0.83 e Å^{-3}. The top peak was associated with H(11A) at a distance of 1.08 A. The next peak with 0.69 e Å^{-3} was near O(5C). In the final cycle, the maximum shift and shift/esd are 0.002 and 0.069, respectively. An extinction correction was refined to 0.001(4). The positional and thermal parameters are given in the Supporting Information.

Physical Measurements. Microanalyses were performed by the Microanalysis Laboratory at the National University of Singapore. Room-temperature magnetic susceptibility measurements were determined on a Johnson-Matthey Magnetic Susceptibility balance MSB-Auto with $Hg[Co(SCN)_4]$ as standard. Corrections for diamagnetism were made using Pascal's constants.[19] Infrared spectra were recorded as KBr disks on a Shimadzu IR 470 infrared spectrophotometer. Electronic transmittance spectra were recorded on a Shimadzu UV-240 spectrophotometer as Nujol mulls. Conductance measurements were made using a Kyoto Electronics CM-115 conductivity meter with a Kyoto Electronics conductivity cell on ca. 1 mM solutions. The ^{1}H NMR spectra were recorded on a Bruker ACF 300 Spectrometer at 300 MHz for solutions in DMSO-d_6 with $SiMe_4$ as internal standard. Formation constants were determined at 25 ± 0.1 °C, spectrophotometrically in 30% DMSO solutions at a compound concentration of 10^{-5} M as a function of measured pH using the program SQUAD.[20] Tables of electronic, conductance, and IR data are given in the Supporting Information.

Results and Discussion

Acylbis(salicylaldehyde hydrazones), H_4L^n, may be considered as two salicylaldehyde hydrazones linked via a methylene chain of variable length. As such there are potentially four ionizable protons, two each from the phenol and the amide moieties. By analogy with salicylaldehyde acetylhydrazone (H_2sa), the H_4L^n ligands can potentially act as hexadentate chelators, binding two Cu(II) ions, one in each tridentate domain. In contrast to H_2sa where addition of nonbasic Cu(II) salts gives monoanionic ligand species $Cu(Hsa)^+$, H_4L^n results in immediate precipitation of $[\{Cu_2L^n\}_m]$ where both the phenolic and amide moieties are deprotonated. This is presumably driven by the

(16) *SMART & SAINT Software Reference Manuals*, Version 4.0; Siemens Energy & Automation, Inc., Analytical Instrumentation: Madison, WI, 1996.
(17) Sheldrick, G. M. *SADABS; Software for empirical absorption correction*; University of Göttingen: Göttingen, Germany, 1996.
(18) *SHELXTL Reference Manual, Version 5.03*; Siemens Energy & Automation, Inc., Analytical Instrumentation: Madison, WI, 1996.
(19) Earnshaw, A. *Introduction to Magnetochemistry*; Academic Press: London, 1968; p 48.

Table 1. Elemental Analysis, Colors, and Effective Magnetic Moments of Complexes

complex	color	analysis (%)[a] C	H	N	μ_{eff}[b]/μ_B
$[\{Cu_2L^0\}_m]\cdot 2mH_2O$	khaki	39.9 (39.6)	2.9 (2.9)	11.8 (11.6)	1.50
$[\{Cu_2L^1\}_m]\cdot 5mH_2O$	brown	36.5 (36.9)	3.6 (4.0)	10.0 (10.1)	1.59
$[Cu_2(H_2L^1)(H_2O)_2]\cdot(ClO_4)_2\cdot 5.5H_2O$[c]	green	25.6 (25.5)	3.5 (3.6)	6.9 (7.0)	1.78
$[\{Cu_2L^2\}_m]\cdot mH_2O$	green	43.4 (43.6)	3.1 (3.3)	11.0 (11.3)	1.49
$[\{Cu_2(H_2L^2)Cl_2\}_m]\cdot 0.5mH_2O$	brown	38.3 (38.6)	2.8 (3.1)	9.7 (10.0)[d]	1.37
$[\{Cu_2(H_2L^2)\}_m]\cdot(ClO_4)_{2m}$	green	31.7 (31.8)	2.5 (2.4)	8.2 (8.3)[e]	1.33
$[\{Cu_2L^4\}_m]\cdot 2.5mH_2O$	green	43.9 (43.6)	4.1 (4.2)	10.0 (10.2)	1.58
$[\{Cu_2(H_2L^4)Cl_2\}_m]\cdot 1.5mH_2O$	green	40.0 (39.7)	3.8 (3.8)	8.8 (9.2) [f]	1.44
$[\{Cu_2(H_2L^4)\}_m]\cdot(ClO_4)_{2m}\cdot 2mH_2O$	green	32.2 (32.3)	3.3 (3.3)	7.4 (7.5) [g]	1.35
$[\{Cu_2(H_2L^4)\}_m]\cdot(ClO_4)_{2m}\cdot m(C_2H_5OH)\cdot 3mH_2O$[h]	green	32.6 (32.8)	4.2 (4.0)	6.8 (6.9)	1.46
$[\{Cu_2L^6\}_m]\cdot 2mH_2O$	green	46.7 (46.4)	4.3 (4.6)	9.7 (9.8)	1.60
$[\{Cu_2(H_2L^6)\}_m]\cdot(ClO_4)_{2m}\cdot 1.5mH_2O$	green	34.7 (34.7)	3.6 (3.6)	7.3 (7.4)[i]	1.33
$[\{Cu_2L^8\}_m]\cdot 2.5mH_2O$	green	47.5 (47.5)	5.1 (5.1)	9.6 (9.3)	1.53
$[\{Cu_2(H_2L^8)Cl_2\}_m]\cdot 6mH_2O$	green	38.9 (38.8)	5.1 (5.4)	7.4 (7.5) [j]	1.84
$[\{Cu_2(H_2L^8)\}_m]\cdot(ClO_4)_{2m}\cdot 2.5mH_2O$	green	35.6 (35.7)	4.3 (4.1)	6.9 (6.9)[k]	1.29
$[\{Cu_2L^{10}\}_m]\cdot 2.5mH_2O$	green	49.3 (49.2)	5.1 (5.5)	8.7 (8.8)	1.68
$[\{Cu_2(H_2L^{10})Cl_2\}_m]\cdot 2.5mH_2O$	green	44.1 (44.1)	5.2 (5.2)	8.3 (7.9) [l]	1.94
$[\{Cu_2(H_2L^{10})\}_m]\cdot(ClO_4)_{2m}\cdot m(C_2H_5OH)$	green	40.5 (40.2)	4.7 (4.6)	7.1 (6.7)[m]	1.32
$[\{Cu_2L^{14}\}_m]\cdot mC_2H_5OH$	green	55.4 (55.5)	6.3 (6.4)	7.9 (8.1)	1.55
$[\{Cu_2(H_2L^{14})\}_m]\cdot(ClO_4)_{2m}\cdot 1.5mH_2O$	green	41.2 (41.2)	4.7 (4.9)	6.1 (6.4)[n]	1.24

[a] Calculated value in parentheses. Satisfactory Cu analyses were obtained for all complexes. [b] At 298 K per metal ion. [c] X-ray structure gives $[Cu_2(H_2L^1)(H_2O)_2]\cdot 2(ClO_4)\cdot 3H_2O$; % Cl, 9.2 (8.9). [d] % Cl, 12.7 (12.4). [e] % Cl, 9.9 (10.5). [f] % Cl, 11.7 (10.7). [g] % Cl, 10.1 (9.6). [h] X-ray structure gives $[\{Cu_2(H_2L^4)(C_2H_5OH)_2\}_m]\cdot(ClO_4)_{2m}\cdot m(C_2H_5OH)$; % Cl, 8.9 (8.8). [i] % Cl, 9.2 (9.3). [j] % Cl, 11.2 (9.6). [k] % Cl, 8.9 (8.8). [l] % Cl, 12.1 (10.0). [m] % Cl, 8.6 (8.5). [n] % Cl, 7.9 (8.1).

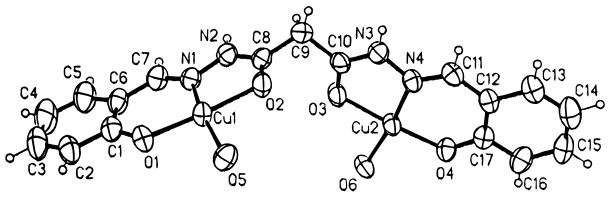

Figure 1. Structure of the monomeric $[Cu_2(H_2L^1)(H_2O)_2]^{2+}$ cation of **1** showing the numbering scheme.

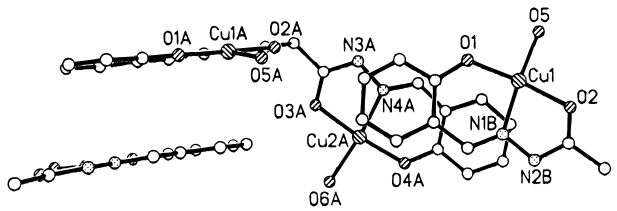

Figure 2. Diagram illustrating the significant π overlap of adjacent cations of **1** to give zigzag chains, with partial numbering only.

very low solubility of the latter complexes in common solvents. However, solubilization does occur in DMSO and certain coordinating solvents.[21] Addition of mineral acid to a suspension of $[Cu_2L^n]$ in ethanol results in dissolution due to protonation of the coordinated ligand and the increased charge on the complex. It proved difficult to control the protonation state of the ligand and therefore to isolate pure material. However, addition of dilute HCl during synthesis gave $[\{Cu_2(H_2L^n)Cl_2\}_m]$ ($n = 2, 4, 8, 10$) or $HClO_4$ gave $[\{Cu_2(H_2L^n)\}_m]\cdot(ClO_4)_{2m}$ ($n > 1$). For other ligands no analytically pure product was isolated. Microanalytical data for all complexes are listed in Table 1 together with colors and magnetic moments.

Crystal Structure of $[Cu_2(H_2L^1)(H_2O)_2]\cdot(ClO_4)_2\cdot 3H_2O$ (1). An ORTEP diagram (with 50% probability thermal ellipsoids) giving the unique atom labeling is shown in Figure 1. Selected bond distance and angle data are given in Tables 2 and 3, respectively. The crystallographically independent Cu(II) centers are square-planar and coordinated by the tridentate ligand domains, with the final site being occupied by water. Bonding data agree with those for related ligands[12,22] and Cu(II) complexes.[5,6] The planar domains are linked via the methylene C9 and are inclined at 80° to each other. Domains from adjacent molecules stack nearly parallel to each other with an average separation of 3.32 Å, resulting in significant π overlap between rings (Figure 2). The Cu(II) centers within a given ligand are 6.390(2) Å apart; however, stacked domains give a separation of 4.14 Å which could facilitate weak interactions.

Table 2. Selected Bond Lengths (Å) for $[\{Cu_2(H_2L^4)(C_2H_5OH)_2\}_m]\cdot(ClO_4)_{2m}\cdot m(C_2H_5OH)$ (**2**) and $[Cu_2(H_2L^1)(H_2O)_2]\cdot(ClO_4)_2\cdot 3H_2O$ (**1**) with Estimated Standard Deviations in Parentheses

	2	**1**		
Cu1−O1	1.901(3)	1.894(4)	Cu2−O4	1.899(4)
Cu1−N1	1.932(3)	1.929(6)	Cu2−N4	1.926(5)
Cu1−O5	1.964(4)	1.955(5)	Cu2−O6	1.958(4)
Cu1−O2	1.978(3)	1.985(4)	Cu2−O3	1.979(5)
Cu1−O1A	2.437(3)	—	—	—
O1−C1	1.336(5)	1.337(9)	O4−C17	1.323(8)
C6−C7	1.435(6)	1.457(10)	C12−C11	1.422(10)
C7−N1	1.295(5)	1.291(8)	C11−N4	1.296(8)
N1−N2	1.393(5)	1.391(8)	N4−N3	1.390(7)
N2−C8	1.343(6)	1.328(9)	N3−C10	1.323(9)
C8−O2	1.252(6)	1.249(8)	C10−O3	1.243(8)
C8−C9	1.503(6)	1.495(9)	C10−C9	1.503(9)
C9−C10	1.516(7)	—	—	—
C10−C10B	1.531(8)	—	—	—
O5−C11	1.414(7)	—	—	—
C11−C12	1.514(6)	—	—	—
Cu···CuA	3.220(1)	6.390(2)	—	—

Crystal Structure of $[\{Cu_2(H_2L^4)(C_2H_5OH)_2\}_m]\cdot(ClO_4)_{2m}\cdot m(C_2H_5OH)$ (2). An ORTEP diagram (with 50% probability thermal ellipsoids) giving the unique atom labeling is shown in Figure 3. Selected bond distance and angle data are given in Tables 2 and 3, respectively. The two monoanionic, tridentate domains of the ligand adopt a trans configuration, and each coordinates a copper(II) ion forming a dimetal complex.

(20) Leggett, D. J.; McBryde, W. A. E. *Anal. Chem.* **1975**, *47*, 1065−1070.
(21) Ranford, J. D.; Vittal, J. J.; Wang, Y. M. Manuscript in preparation.
(22) Zhang, X. M.; You, X. Z. *Polyhedron* **1996**, *15*, 1793−1796.

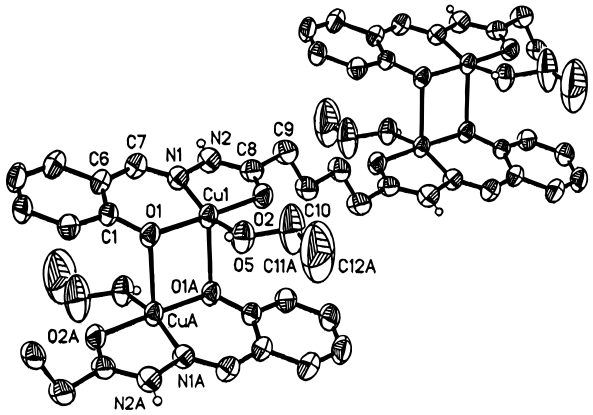

Figure 3. Structure of polymeric $[\{Cu_2(H_2L^4)(C_2H_5OH)_2\}_m]^{2+}$ and symmetry-related cations of **2** showing the numbering scheme.

Table 3. Selected Bond Angles (deg) for $[\{Cu_2(H_2L^4)(C_2H_5OH)_2\}_m]\cdot(ClO_4)_{2m}\cdot mC_2H_5OH$ (**2**) and $[Cu_2(H_2L^1)(H_2O)_2]\cdot(ClO_4)_2\cdot 3H_2O$ (**1**) with Estimated Standard Deviations in Parentheses

	2	**1**		
O1−Cu−N1	92.5(1)	93.2(2)	O4−Cu2−N4	92.9(2)
O1−Cu−O2	173.6(1)	174.3(2)	O4−Cu2−O3	173.9(2)
O1−Cu−O5	90.4(2)	93.9(2)	O4−Cu2−O6	94.3(2)
O1−Cu−O1A	85.0(1)	—	—	—
N1−Cu−O2	81.9(1)	81.2(2)	N4−Cu2−O3	81.1(2)
N1−Cu−O5	161.6(2)	168.9(2)	N4−Cu2−O6	171.4(2)
N1−Cu−O1A	108.4(1)	—	—	—
O2−Cu−O5	95.9(2)	91.9(2)	O3−Cu2−O6	91.6(2)
O2−Cu−O1A	94.0(1)	—	—	—
O5−Cu−O1A	89.9(2)	—	—	—
Cu−O1−C1	126.0(3)	126.8(4)	Cu2−O4−C17	127.5(4)
Cu−O1−CuA	95.1(1)	—	—	
C1−O1−CuA	113.2(2)	—	—	
O1−C1−C2	117.6(4)	118.3(7)	O4−C17−C16	118.4(6)
O1−C1−C6	124.4(3)	124.5(6)	O4−C17−C12	124.1(6)
C1−C6−C7	123.7(4)	124.3(6)	C17−C12−C11	123.6(6)
C5−C6−C7	117.4(4)	116.8(7)	C13−C12−C11	117.4(7)
C6−C7−N1	122.7(4)	121.6(6)	C12−C11−N4	123.7(6)
C7−N1−Cu	128.8(3)	129.4(5)	C11−N4−Cu2	128.3(5)
C7−N1−N2	120.0(4)	118.9(6)	C11−N4−N3	120.3(6)
N1−N2−C8	114.8(3)	114.4(5)	N4−N3−C10	114.6(5)
N2−N1−Cu	111.0(3)	111.6(4)	N3−N4−Cu2	111.4(4)
N2−C8−O2	120.1(4)	120.6(6)	N3−C10−O3	120.5(6)
N2−C8−C9	117.5(4)	118.6(6)	N3−C10−C9	118.9(6)
C8−O2−Cu	112.2(3)	112.2(4)	C10−O3−Cu2	112.3(4)
O2−C8−C9	122.4(4)	120.7(6)	O3−C10−C9	120.6(6)
C8−C9−C10	111.8(4)	110.2(6)	—	—
C9−C10−C10B	111.5(5)	—	—	—
Cu−O5−C11	125.5(4)	—	—	—
O5−C11−C12	119.1(7)	—	—	—

Centrosymmetric, axial phenolato (O1) bridges link adjacent domains into a linear stepped polymer giving a Cu···Cu separation of 3.220(1) Å. The structure[5] of $[\{Cu(Hsa)(py)(NO_3)\}_2]$ also has such a dimeric stacked arrangement but with a weaker axial interaction, thereby resulting in a Cu···Cu distance of 3.610(2) Å. The Cu(II) ion is coordinated in the plane by a tridentate ligand domain and a bound ethanol molecule. A more weakly bound bridging phenolate (Cu−O1A, 2.437(3) Å) completes the coordination sphere in an axial site. The in-plane and ligand metric parameters may be considered normal, vide supra. The polymeric chain extends approximately along the [011] plane and stacks along the *a* axis with ClO and ethanol solvate filling the gap.

Physicochemical Studies. The position of the ligand to Cu(II) charge-transfer transition for complexes with $n > 0$ fall in the range 380−420 nm and is typical for acylhydrazones[9,13b] and arylhydrazones.[6] For $[\{Cu_2L^0\}_m]\cdot 2mH_2O$ this transition occurs at lower energy (450 nm), possibly a result of the extended conjugation possible in this ligand. Lal et al. reported[15] this transition for $[Cu_2L^0]\cdot 4H_2O$ at 355 nm where we find only a number of ligand internal transitions. The d−d transitions generally fall below 700 nm and are more consistent with square-pyramidal and square-planar geometries[23] about the Cu(II) as seen for **1** (650 nm) and **2** (650 nm) and related complexes.[5,6] The exception is $[\{Cu_2(H_2L^2)Cl_2\}_m]\cdot 0.5mH_2O$ (730 nm) which is likely to be tetragonal, indicating axial ligand coordination of anion or solvent.[5,6]

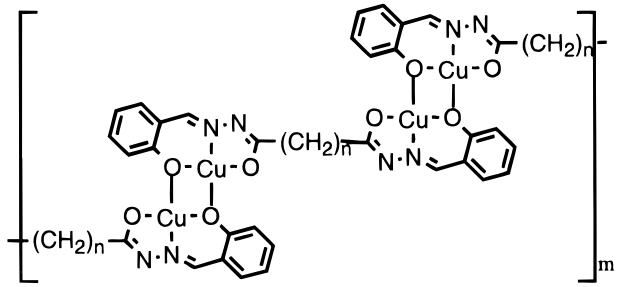

Figure 4. Proposed structure for oligomeric $[\{Cu_2L^n\}_m]$.

Most complexes display low magnetic moments (Table 1) indicative of antiferromagnetic interactions. Analogues H_2sa[5] and H_2sb[6] with Cu(II) and structurally related systems[7] often adopt dimeric, phenolato bridged structures which all have abnormal μ_{eff} values. The ligands in this study have two tridentate domains, therefore the complexes formed are likely to be based on oligomeric chains with bridging phenolates, as shown in Figure 4. This would give Cu···Cu separations of ca. 3 Å with a coplanar geometry favoring magnetic orbital overlap. The trans arrangement, as depicted, is likely to exist for short methylene chains due to steric interactions between aromatic rings as seen in **2** (Figure 3). The structure of **1** has monomeric Cu(II) ions (Figure 1) which are magnetically dilute, accounting for the normal magnetic moment (1.78 μ_B). Magnetic data for **2** were unreliable due to rapid complex decomposition.

Dianionic ligand complexes with perchlorate have molar conductivity values indicating 1:1 or greater electrolyte behavior. The crystal structures of **1** and **2** have nonbonded ClO_4 indicating that partial association of perchlorate with complex may occur in DMSO solution. For the chloro anion complexes ($[Cu_2(H_2L^n)Cl_2]$; $n = 2, 4, 8, 10$), molar conductivity values indicate partial ionization only, therefore the anions are formulated as bound, presumably in axial sites due to the low magnetic moments. All tetraanionic complexes are nonelectrolytes.

The possibility of Cu(II) interacting with more than one tridentate domain, either from two different ligands or from the two ends of one ligand folding back, is not expected. Attempts to form such compounds for these ligands as well as H_2sa and H_2sb have all been unsuccessful, due presumably to the restricted bite angle of the binding domain coupled with the Jahn−Teller distortions for Cu(II), which would require the second binding domain to have longer apical interactions.

The ligands show IR bands assigned to ν(OH) (ca. 3300 cm^{-1}), ν(C═O) (1647−1667 cm^{-1}), and ν(C═N) + amide (**II**) (1521−1619 cm^{-1}). As well, aliphatic ν(CH), which is not observed for H_4L^0, becomes progressively more intense as the length of the methylene chain increases. On complexation the ν(C═O) and ν(C═N) + amide (**II**) bands for the dianionic

(23) Lever, A. B. P. *Inorganic Electronic Spectroscopy*; Elsevier: Amsterdam, 1984.

Table 4. Protonation and Formation Constants with Cu(II) for Selected Ligands[a]

	pK_n				
	ligand[b]				Cu(II)[c]
	pK_1	pK_2	pK_3	pK_4	pK
H_4L^1	14.5(1)	12.7(1)	9.3(2)	6.7(3)	19.0(2)
H_4L^2	14.4(1)	13.4(1)	9.2(1)	6.8(1)	18.1(1)
H_4L^4	14.2(1)	12.4(2)	9.2(2)	6.9(2)	17.9(1)
H_4L^8	14.5(1)	12.6(2)	9.3(2)	7.2(3)	18.3(1)
H_2as	—	13.6(1)	—	9.1(1)	16.2(2)
H_2sb[d]	—	9.11(4)	—	6.77(4)	—
H_2pb[d]	—	11.40(4)	—	7.68(4)	—

[a] All work carried out at 25.0 ± 0.1 °C. Values obtained from electronic spectra. [b] H_4L^n: pK_1, $H^+ + L^{4-} = HL^{3-}$; pK_2, $H^+ + HL^{3-} = H_2L^{2-}$; pK_3, $H^+ + H_2L^{2-} = H_3L^-$; pK_4, $H^+ + H_3L^- = H_4L$. H_2as, H_2sb, H_2pb: pK_1, $H^+ + L^{2-} = HL^-$; pK_2, $H^+ + HL^- = H_2L$. [c] $Cu^{2+} + L = CuL$. [d] From ref 25. Formation constants with Cu(II) not reported.

ligands shift, showing that coordination involves the carbonyl O and imine N. For the tetraanionic ligands these bands shift and split, being characteristic for this type of ligand and indicating the formation of a diimine-like moiety[5,6] (see Figure 4). These results indicate that the ligand exists in a keto form in the solid state but that on metal binding the deprotonated chelator has considerable enol character.

Because of the biological activity of these compounds[24] and the important role Cu(II) plays in this activity, the protonation constants for selected ligands (H_4L^n, with $n = 1$, 2, 4, 8, and H_2as) and their formation constants with Cu(II) were determined (Table 4). Due to poor aqueous solubility of the ligands, formation constants were investigated spectrophotometrically in 30% DMSO (the minimum at which all ligands stayed in solution over the pH ranges investigated) at a concentration of 10^{-5} M and are thus tentative. Four ionization processes are observed for the H_4L^n ligands. Although the two tridentate domains of the ligands are separated via a methylene linker, the pK values of the pairs of equivalent protons (pK_1 and pK_2; pK_3 and pK_4) do not start to converge with increasing linker length. The first phenolic proton is most acidic with an average pK_4 of 6.9, indicating that at a physiological pH of 7.4 the ligands exist predominantly as $(H_3L^n)^-$. The second phenol proton has a mean pK_3 value of 9.25, which is 2.35 pK units higher than pK_4. For H_2as the first ionization has a pK of 9.1, significantly higher than H_4L^n and similar to pK_3, whereas for H_2sb and H_2pb (pyridoxal benzoylhydrazone) these are 6.77 and 7.68, respectively,[25] consistent with these ligands higher degree of conjugation and stabilization of the resultant anion. A study[26] of H_4L^n ($n = 1$, 2, 3) in 95% DMF gave pK_1 and pK_2 values separated by ca. 0.2 log units with an average value of 7.8. The amide protons have average pK_2 and pK_1 values of 12.8 and 14.4, respectively, comparable to H_2as (13.6); for H_2sb and H_2pb this is reduced (9.11 and 11.40, respectively).

Protonation constants and pK_2 for the di-Cu(II) complexes could not be assessed accurately due to complex precipitation above ca. pH 7; however, chemical properties show chelation with Cu(II) results in the phenol becoming a strong acid and the amide requiring the presence of dilute mineral acid to ensure its protonation. The average stability constants of 18.1 for pK_1 show the ligands to bind Cu(II) strongly, as expected for such a tridentate, dianionic domain. The reported[26] average stability constants in 95% DMF of Cu(II) with H_4L^n ($n = 1$, 2, 3) of 4.3 for pK_1 and 3.3 for pK_2 therefore seem unreasonably low.

Conclusions

H_4L^n ligands have two tridentate metal binding domains. We have prepared dicopper(II) complexes of both the di- and tetraanionic forms of the antitumor ligand analogues H_4L^n. Polymeric complexes predominate, with copper domains being either stacked, as found in $[\{Cu_2(H_2L^4)(C_2H_5OH)_2\}_m]\cdot(ClO_4)_{2m}\cdot m(C_2H_5OH)$, or adopting a side-by-side arrangement, consistent with the antiferromagnetic magnetic exchange coupling observed. Monomeric structures are also possible as seen for $[Cu_2(H_2L^1)(H_2O)_2]\cdot(ClO_4)_2\cdot 3H_2O$ where significant π overlap between planar, metal binding domains occurs. The magnetic moment for the monomeric complex is normal, and may be tentatively used to give information on complex geometry. Proton stability constant data shows the ligands would exist predominately as monoanions at physiological pH. On complexation to Cu(II) the very weakly acidic amide protons are sufficiently acidic to require the presence of mineral acid to ensure their protonation. The planar, tridentate domain coupled with Jahn−Teller distortions for Cu(II) allow only one domain to bind per metal. This may play an important role in the biological activity of such species when compared to metals which will form octahedral complexes.

Acknowledgment. Support for this work by the National University of Singapore (Grant RP 950651) is greatly appreciated.

Supporting Information Available: Tables detailing the X-ray data collection and refinement, complete positional and thermal parameters, atomic coordinates, bond distances and angles, anisotropic thermal parameters, torsion angles, and hydrogen atom coordinates for **1** and **2**, and IR, electronic, and molar conductance data (24 pages). Ordering information is given on any current masthead page.

IC970805G

(24) Lian, K. O.; Long, Y. C.; Ranford, J. D.; Wang, Y. M. Manuscript in preparation.

(25) (a) Dubois, J. E.; Fakhrayan, H.; Doucet, J. P.; El Hage Chahine, J. M. *Inorg. Chem.* **1992**, *31*, 853−859. (b) Fakhrayan, H.; Doucet, J. P.; El Hage Chahine, J. M. *Bull. Soc. Chim. Belg.* **1993**, *102*, 377−389.

(26) Cho, H. K.; Cha, B. H.; Hur, Y. A.; Choi, K. S. *J. Kor. Chem. Soc.* **1995**, *39*, 281−287.